Pis'ma v ZhETF, vol. 83, iss. 1, pp. 41 – 45 © 2006 January 10

Equation of State and High Pressure Irreversible Amorphization in $Y_3Fe_5O_{12}$

A. G. Gavriliuk[+*△], *V. V. Struzhkin*[+], *I. S. Lyubutin*[1)△], *M. I. Eremets*[□], *I. A. Trojan*[*], *V. V. Artemov*[△]

[+] *Geophysical Laboratory, Carnegie Institution of Washington, 5251 Broad Branch Road NW, Washington DC 20015*

[*] *Institute for High Pressure Physics RAS, 142190 Troitsk, Moscow reg., Russia*

[△] *Institute of Crystallography RAS, 119333 Moscow, Russia*

[□] *Max-Planck Institut fur Chemie, 55020 Mainz, Germany*

Submitted 17 November 2005

The change of crystal structure in the yttrium iron garnet $Y_3Fe_5O_{12}$ was studied at room temperature at high pressures up to ~ 55 GPa by the X-ray diffraction technique in diamond anvil cells. At the pressure about ~ 50 GPa the drastic change in the X-ray diffraction pattern was observed indicating a transition into an amorphous-like state. At the pressure increase the bulk modulus of YIG was found to be 193 ± 4 GPa. It was also found that the amorphous state was retained after decompression down to ambient pressure. From the shape of X-ray patterns in "amorphous" phase, it was concluded that the local atomic structure consists of iron-oxygen FeO_6 octahedral complexes with disordered orientations of local axis and of the randomly arranged others ions fragments with the overall $Y_3Fe_5O_{12}$ composition. For amorphous phase it was evaluated that the bulk modulus of FeO_6 octahedral complexes is about 260 GPa.

PACS: 61.50.Ks, 64.30.+t, 71.30.+h, 81.40.Vw

Introduction. The yttrium iron garnet (YIG) $Y_3Fe_5O_{12}$ belongs to a well-known class of rare-earth iron garnets which are ferrimagnets [1 – 3] with dominant antiferromagnetic interaction. Its Neel temperature is about 559 K at ambient pressure. It has the cubic crystal structure with space group $Ia{-}3d$, and the unit cell parameter at normal conditions is $a_0 = 12.3738$ Å [4]. In the unit cell, Fe^{3+} ions occupy two different sites, with octahedral and tetrahedral oxygen environments. Schematic picture of arrangement of octal and tetra polyhedra in YIG is shown in Fig.1. The polyhedra form an alternating three-dimensional network where all corners of tetrahedrons are common corners of nearest neighbor octaherda and wise versa. These different sites of iron ions build two different magnetic sub-lattices with opposite directions of magnetization. Two Fe^{+3} ions from octahedral sites partially compensate magnetization of three Fe^{+3} ions from tetrahedral sites giving $5\mu_B$ of the total magnetization per formula unit [1].

Recently, an electronic transition with possible metallization of YIG was discovered in the pressure range $40 \div 50$ GPa [5]. At this transition, the optical gap in YIG drastically decreases from ~ 2.3 eV to almost zero value. At decompression, the back transition was not completely reversible. This transition was also accompanied by a possible crystal amorphization, as follows from Urbach shape of the absorption edge [6, 7] and from previous investigations of the amorphous state of YIG [7]. The high-pressure Mossbauer spectra indicated the magnetic collapse at $P \approx 50$ GPa, and in the high-pressure nonmagnetic phase of YIG the spectra are similar to those in the amorphous state of YIG [8].

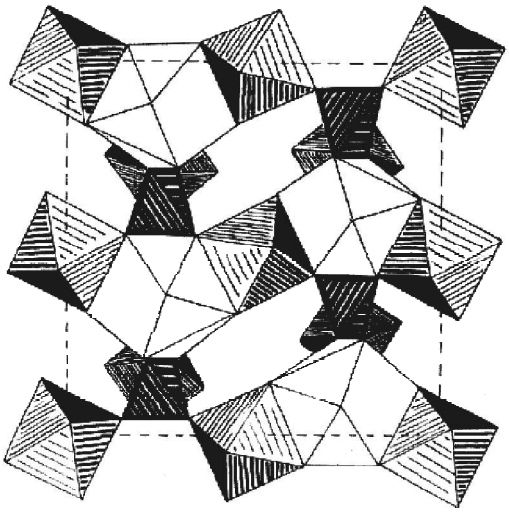

Fig.1. Schematic view of crystal structure of $Y_3Fe_5O_{12}$. Octahedral and tetrahedral iron- oxygen polyhedra are shaded. The dodecahedral sites of Y ions are also clearly seen

[1)] e-mail: lyubutin@ns.crys.ras.ru

In the present study, external high pressures were applied to the YIG powder sample to modify its crystal structure and to observe possible structural transitions. The measurement of X-ray diffraction patterns was used to investigate changes in the crystal structure parameters of YIG in diamond anvil cells at pressure increase and at decompression. The room temperature equation of state (EOS) was measured at compression, which gives a possibility, in combination with the other techniques, to interpret high-pressure behavior of electronic and magnetic properties of the material.

Experiment. The X-ray structural studies were performed under high pressures up to 55 GPa at room temperature in a diamond anvil cell. The high-quality $Y_3Fe_5O_{12}$ single crystal film with thickness $\sim 7.5\,\mu$m was grown on a $Ga_3Al_5O_{12}$ substrate in the (111) direction and then it was cleaved from the substrate. A few crystals were grinded to fine powder in an agate mortar to the average grain size of no more than one micron. Then, as prepared $Y_3Fe_5O_{12}$ powder, was placed into the hole in the rhenium gasket of the high-pressure cell with diamond anvils. The diameter of the working surface of diamonds in the cell was about $\sim 400\,\mu$m and the diameter of the hole in the rhenium gasket, where the sample was placed, was about $120\,\mu$m. Silicon-organic liquid PES-5 (poly-ethil-siloxane) was used as a pressure medium. The volume of the sample was no more than 1/3 of the working volume of the cell and 2/3 of the cell volume was filled with pressure medium. The high-pressure cell allowed the detection of diffraction reflections up to the angles $2\Theta = 18°$. Experiments were carried out at the APS (Argonne, USA, beamline 16-IDB) and at ESRF (Grenoble, France, beamline ID30) synchrotron X-ray sources in the angle dispersion mode with X-ray beam-spot focused down to $10\times10\,\mu m^2$. The spectra were measured in the transmission geometry by a two-dimensional detector of the fast Image-Plate type (MAR345). The pressure was determined by the standard ruby fluorescence technique. Several ruby chips with dimensions 1–5 μm were placed into the cell at different distances from the center of the hole to evaluate the pressure distribution. The gradient was found to be no higher than 4–5 GPa at maximum pressure.

Results and discussion. The X-ray diffraction pattern of the as prepared initial powder sample $Y_3Fe_5O_{12}$ shows a standard picture of reflexes corresponding to the garnet structure of $Ia{-}3d$ space group [9]. The evolution of the X-ray patterns obtained at pressure increase up to $\sim$ 50 GPa is shown in Fig.2. With compression, all peaks shift toward the greater angles and become a little bit broader (presumably, due to the growing pressure gradient). In the pressure interval

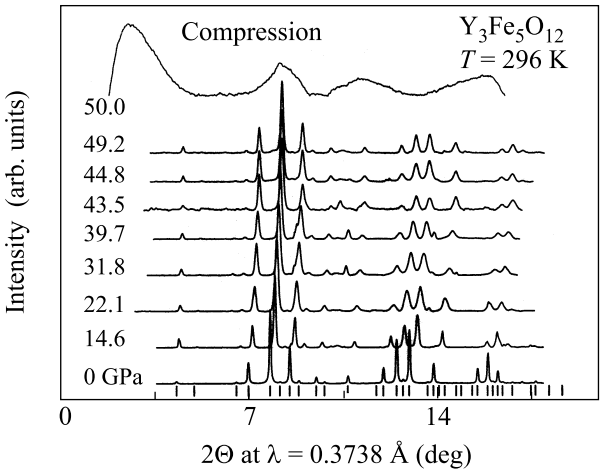

Fig.2. Evolution of the X-ray diffraction patterns for $Y_3Fe_5O_{12}$ at pressure increase. Strokes at bottom are the reflex positions of the garnet structure taken from the database PDF-2 Ref. [9]

$P \sim 49{-}50$ GPa, all sharp reflexes disappear, indicating a structural transition to an amorphous-like state. At 50.0 GPa, the X-ray pattern demonstrates a few very broad picks, which are typical of an amorphous state (Fig.2).

Figure 3 shows the pressure dependence of the unit cell volume $V(P)$ of the garnet. For the pressure increase regime, the experimental points were approximated by

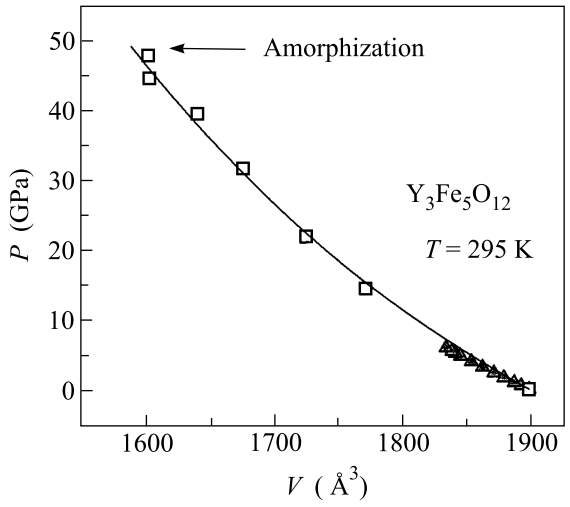

Fig.3. The pressure dependence of the relative volume of the unit cell of $Y_3Fe_5O_{12}$ during compression. The symbols correspond to experimental points at increasing pressure. Open symbols – experimental data from this study, gray triangles – data from Ref. [12]. Solid line is the fit to the Burch–Murnaghan equation of states

the Birch–Murnaghan [10, 11] equation of state

$$P(V) = \frac{3B_0}{2}\left[\left(\frac{V}{V_0}\right)^{-7/3} - \left(\frac{V}{V_0}\right)^{-5/3}\right] \times$$

$$\times \left\{1 + \frac{3}{4}(B_0' - 4)\left[\left(\frac{V}{V_0}\right)^{-2/3} - 1\right]\right\}. \qquad (1)$$

From the approximation we evaluated the value of bulk elastic modulus $B_0 = 193 \pm 4$ GPa, with its derivative $B_0' = 4$ (fixed), and the unit cell volume of YIG at the normal pressure $V_0 = 1897.4\,\text{Å}^3$. These data agree well with previous measurements [12].

The most important effect is the abrupt disappearance of the sharp crystalline X-ray reflexes at ~ 50 GPa. This disappearance is very sharp which suggests a possibility of first-order type transition from the crystalline to an amorphous-like sate. As it was shown recently from the optical spectra [5], the electronic transition with a possible metallization of YIG is also takes place in this region of pressures.

From the analysis of evolution of diffraction patterns in the amorphous phase of YIG at decompression (Fig.4) and from the careful analysis of interionic distances in

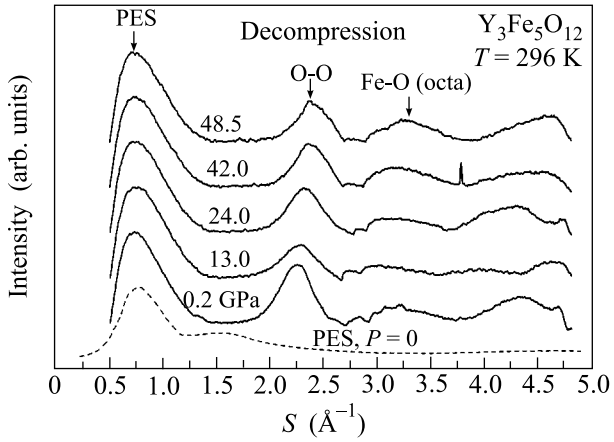

Fig.4. Evolution of X-ray diffraction patterns for amorphous $Y_3Fe_5O_{12}$ at decompression

the initial crystalline YIG, we suggested the assignments of broad picks in diffraction patterns of the amorphous phase. We draw X-ray patterns with the X-coordinate as $S = 4\pi \sin\theta/\lambda$ (see Fig.4) which is accepted for analysis of the X-ray diffraction in amorphous materials. The first strongest pick at about $S \approx 0.75\,\text{Å}^{-1}$ is attributed to diffraction from the PES (poly-ethil-siloxane) compound. Diffraction pattern from PES at ambient pressure is shown as dashed line in Fig.4 [13]. The position of the PES's pick is almost independent of pressure. This is easy to recognize if one takes into account that PES liquid is a mixture of polymer molecules of nearly one dimensional structure [14]:

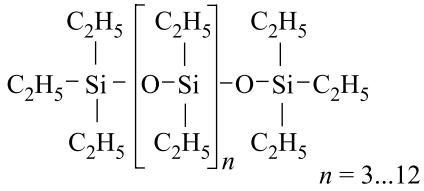

The X-ray pick from PES is determined by the specific dimension of such molecular chains [13]. Non-sensitivity of the X-ray pattern to pressure indicates that the characteristic dimension of the molecules chains does not change and only inter-chain distances can decrease with pressure.

The interionic distances R in the crystalline YIG and in the highly-compressed "amorphous" phase of YIG, calculated from a standard formula $R = \lambda/2\sin(\theta) = 2\pi/S$, are given in Table. A simple analysis shows that the second pick of the "amorphous" phase in Fig.4 at $S \approx 2.3\,\text{Å}^{-1}$ corresponds to $R \approx 2.795$ Å and it is most probably related to the O–O distances of the iron-oxygen FeO_6 octahedrons (see Table and Fig.4). This implies that in the "amorphous" phase of YIG the shape of that pick is maintained by the local FeO_6 octahedral units, which are the dominant characteristic of the amorphous state. This correlates with recent Mossbauer spectroscopy studies [8]. It was concluded from the behavior of the isomer shift of Mossbauer lines that all iron ions acquire the octahedral environment above the critical pressure and preserve it after decompression to ambient pressure [8].

Interionic distances (in Å) in a crystalline YIG as compared with those obtained in the highly-compressed "amorphous" state of YIG at ambient pressure (from pick 1 and pick 2)

Crystalline YIG				
O-O octa	Fe-O octa	O-O tetra	Fe-O tetra	Y-O
2.694	2.020	3.144	1.864	2.356
3.011		2.834		2.434
Amorphous YIG after decompression				
pick 1	pick 2			
2.795	2.020			

Because of the huge background from scattered X-ray photons of synchrotron radiation, only first and second picks of Fig.4 are reliable after background subtraction. The rest of the peaks may be artefacts of calculation procedure. Nevertheless we have also cal-

culated the behavior of the third pick and found that its S value as well as its pressure behavior are very appropriate to the diffraction related to the Fe–O distance of the iron-oxygen octahedron, supporting previous conclusion. Pressure dependencies of the O–O and Fe–O distances are shown in Fig.5a as calculated

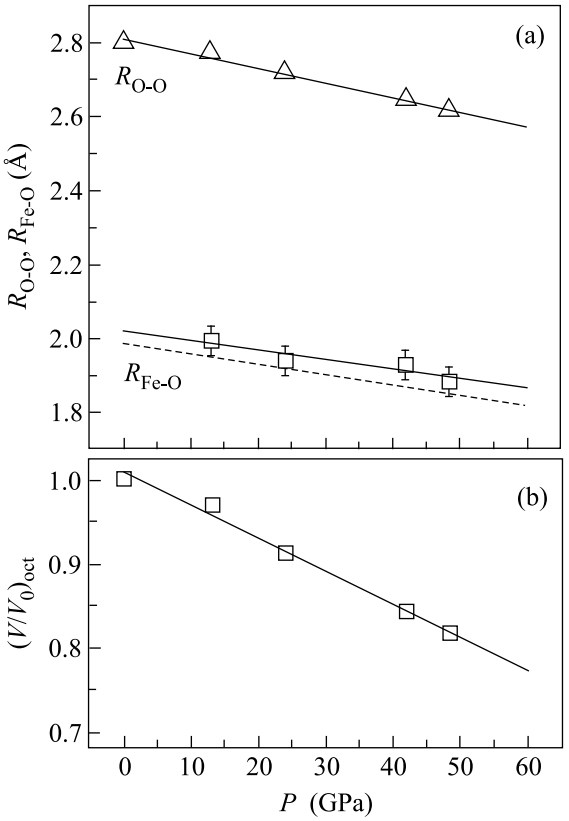

Fig.5. The pressure dependence of the interionic O–O, Fe–O distances (a) and of the relative volume (b) in the iron-oxygen FeO_6 octahedral complex of "amorphous" $Y_3Fe_5O_{12}$ at decompression. The symbols correspond to experimental points. Solid lines are the fits to linear functions, dashed line is the calculation of predicted line for Fe–O distance on the bases of pressure dependence of O–O distance (see text)

from pressure dependencies of the second and third peaks in Fig.4. Then, we fit the experimental points for the pressure dependence of the O–O distance to a linear function (solid line in Fig.5a), and we calculated the Fe–O distances (dashed line in Fig.5a) by formula $R_{Fe-O} = R_{O-O}/\sqrt{2}$ proceed from the geometry of an undistorted octahedron. It turned out that these calculated Fe–O distances are in a good agreement with experimental points.

The solid line in Fig.5a is the linear fit to experimental points. Deviation of the predicted (dashed) line from the experiment could be explained by the distortion of the oxygen octahedra and by uncertainty in determination of the Fe–O distances from the diffraction patterns. The pressure dependence of the relative volume of the iron-oxygen FeO_6 octahedral complex is shown in Fig.5b. From the linear fit, we found that the bulk modulus B_0 of these octahedra is about 260 ± 15 GPa which is in a nice agreement with estimates by other researchers $\sim$ 280 GPa [15], and it is essentially higher than the B_0 value of the initial YIG (193 GPa).

However, our additional investigations in the scanning electron microscope showed that the problem of amorphization of YIG under high pressure is not yet completely clear. The electron microscope images of the $Y_3Fe_5O_{12}$ single crystal plate (Fig.6) indicate that after compression to 61 GPa the crystal plate remains undefeated but it decrepitates into small blocks of square-cubic form with the characteristic dimensions of about 1–2 microns. This resembles the appearance of microtwin domains. The size of such domains is big enough in order to form an ordinary diffraction pattern in the X-ray spectrum. It is hard to perceive that each block or domain of Fig.6b has a glass type structure. May be EXAFS and HRETM investigations will clarify this unusual situation.

Simultaneously with the structural transition, the transition of iron ions from the high- spin to the low-spin state is possible, analogous to the phenomenon that was recently observed in several complex iron oxides in the pressure range of 30–50 GPa [16 – 19]. But this hypothesis needs additional experimental investigation. An additional information about structure before and after transition, about spin states of the ions, and magnetic properties can be obtained from the high-pressure Mössbauer absorption, NFS (nuclear forward scattering), and high resolution X-ray emission spectroscopy (XES) [20] technique. These types of experiments are in our nearest plan.

This work is supported by the DOE grant # DE-FG02-02ER45955, by the Russian Foundation for Basic Research grants # 04-02-16945-a and # 05-02-16142-a, and by the Program of Physical Branch of the Russian Academy of Sciences under the Project "Strongly correlated electronic systems". Use of the HPCAT facility was supported by DOE-BES, DOE-NNSA (CDAC), NSF, DOD -TACOM, and the W.M. Keck Foundation. HPCAT is a collaboration among the Carnegie Institution, Lawrence Livermore National Laboratory, the University of Hawaii, the University of Nevada Las Vegas, and the Carnegie/DOE Alliance Center (CDAC). We thank the HPCAT staff Daniel Hausermann and Peter Liermann for valuable assistance.

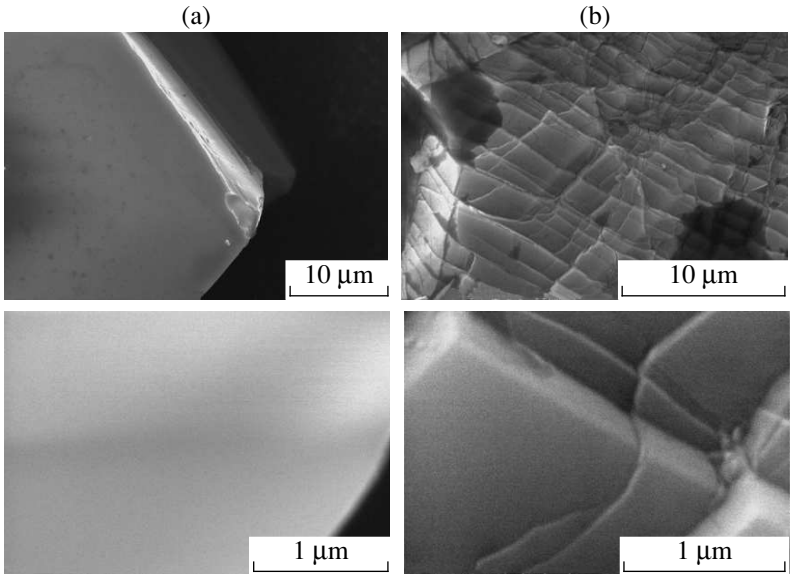

Fig.6. Scanning electron microscopy images of $Y_3Fe_5O_{12}$ single crystal plate, obtained at ambient conditions: (a) before compression, (b) after compression to 61 GPa

1. Charles Kittel, *Introduction to Solid State Physics*, 4 ed., John Wiley and Sons, Inc., New York, London, Sydney, Toronto, 1971.
2. L. Neel, R. Pauthenet, and B. Dreyfus, Progress in Low Temp. Phys. **4**, 344 (1964).
3. S. Geller, J. P. Remeika, R. C. Sherwood et al., Phys. Rev. **137**, A1034 (1965).
4. D. Rodic, M. Mitric, R. Tellgren et al., J. of Magn. and Magn. Mat. **191**, 137 (1999).
5. A. G. Gavriliuk, V. V. Struzhkin, I. S. Lyubutin et al., JETP Letters, submitted (2005).
6. N. F. Mott and E. A. Davis, *Electronic Processes in Non-Crystalline Materials*, 2nd ed., Clarendon Press, Oxford, 1979.
7. E. M. Gyorgy, K.Nassau, M. Eibschutz et al., J. Appl. Phys. **50**, 2883 (1979).
8. I. S. Lyubutin, A. G. Gavriliuk, I. A. Trojan et al., JETP Letters **82** (11) (2005).
9. J. Rosenstingl, E. Irran, C. Hoffmann et al., PDF-II #43. 0507 (1992).
10. F. D. Murnaghan, Proc. of the National Academy of Sciences **30**, 244 (1944).
11. Francis Birch, Phys. Rev. **71**, 809 (1947).
12. F. Sayetat, Thesis, Universite de Grenoble, (unpublished) (1974).
13. A. F. Scryshevskii, *Structural analisis of liquids and amorphous substancies*, II ed. High School, Moscow, 1980.
14. State Standard **13004-77** (1977).
15. R. M. Hazen and L. W. Finder, *Comparative Crystal Chemistry*, Wiley, New York, 1982.
16. A. G. Gavriliuk, I. A. Troyan, R. Boehler et al., JETP Letters **77**, 619 (2003).
17. A. G. Gavriliuk, I. A. Trojan, I. S. Lyubutin et al., JETP **100**, 688 (2005).
18. A. G. Gavriliuk, S. A. Kharlamova, I. S. Lyubutin et al., JETP Letters **80**, 426 (2004).
19. A. G. Gavriliuk, V. V. Struzhkin, I. S. Lyubutin et al., JETP Letters **82**, 243 (2005).
20. J. Badro, G. Fiquet, V. V. Struzhkin et al., Phys. Rev. Lett. **89**, 205504 (2002).